HHS Public Access

Author manuscript

Nat Cell Biol. Author manuscript; available in PMC 2015 January 01.

Published in final edited form as:

Nat Cell Biol. 2014 July ; 16(7): 663–672. doi:10.1038/ncb2988.

The Kinesin-4 Protein KIF7 Regulates Mammalian Hedgehog Signaling by Organizing the Cilia Tip Compartment

Mu He[1,2], **Radhika Subramanian**[3], **Fiona Bangs**[1], **Tatiana Omelchenko**[4], **Karel F. Liem Jr.**[1,5], **Tarun M. Kapoor**[3], and **Kathryn V. Anderson**[1]

[1]Developmental Biology Program, Sloan-Kettering Institute, Memorial Sloan-Kettering Cancer Center, 1275 York Avenue, New York, NY 10065

[2]Program in Biochemistry & Structural Biology, Cell & Developmental Biology, and Molecular Biology, Weill Cornell Graduate School of Medical Sciences, Cornell University, 1300 York Avenue, New York NY 10065 USA

[3]Laboratory of Chemistry and Cell Biology, The Rockefeller University, 1230 York Avenue, New York, NY 10065, USA

[4]Cell Biology Program, Sloan-Kettering Institute, Memorial Sloan-Kettering Cancer Center, 1275 York Avenue, New York, NY 10065

Abstract

Mammalian Hedgehog (Hh) signal transduction requires the primary cilium, a microtubule-based organelle, and the Gli/Sufu complexes that mediate Hh signaling are enriched at cilia tips. KIF7, a kinesin-4 family protein, is a conserved regulator of the Hh signaling pathway and a human ciliopathy protein. Here we show that KIF7 localizes to cilia tips, the site of microtubule plus-ends, where it limits cilia length and controls cilia structure. Purified recombinant KIF7 binds the plus-ends of growing microtubules *in* vitro, where it reduces the rate of microtubule growth and increases the frequency of microtubule catastrophe. KIF7 is not required for normal intraflagellar transport or for trafficking of Hh pathway proteins into cilia. Instead, a central function of KIF7 in the mammalian Hh pathway is to control cilia architecture and to create a single cilia tip compartment where Gli/Sufu activation can be correctly regulated.

Introduction

Although kinesin motor proteins are best known for their roles in intracellular transport, some kinesins can shape the microtubule cytoskeleton by regulating the dynamics of tubulin polymerization. For example, KIF4A, a kinesin-4 protein, controls microtubule length during cell division [1–4] and another kinesin-4 protein, KIF21A, inhibits microtubule growth at the cell cortex [5]. KIF7, a conserved regulator of Hedgehog (Hh) signaling [6–9], is also a member of the kinesin-4 family but its relationship to microtubules has not been defined.

[5]Current address: Vertebrate Developmental Biology Program, Dept. of Pediatrics, Yale School of Medicine, New Haven, CT 06520

The Hedgehog signaling pathway is an evolutionary conserved pathway responsible for many aspects of embryonic development and stem cell maintenance, and is disrupted in a spectrum of tumors[1011]. *Drosophila* Costal2 (Cos2) and its mammalian homologue KIF7 are required to relay the signals from the membrane protein Smoothened (Smo) to the transcription factors of the Ci/Gli family. Genetic inactivation of either *Cos2* or *Kif7* causes a relatively mild ectopic activation of Hh signaling due to their roles in production of both activator and repressor forms of Ci/Gli proteins[11,12]. Recessive mutations in human *KIF7* are associated with fetal hydrolethalus, and acrocallosal and Joubert syndromes; affected individuals exhibit polydactyly, brain abnormalities and cleft palate, consistent with a role for KIF7 in human Hh signaling [13,14].

A fundamental difference between the *Drosophila* and vertebrate Hh pathways is the dependence of vertebrate Hh signaling on a microtubule-based organelle, the primary cilium [15]. Mutations that block formation of primary cilia prevent cellular responses of cells to Hedgehog ligands, and all of the proteins required for vertebrate Hh signal transduction are highly enriched in cilia and change localization in response to ligand [16]. The activity of KIF7 in the mouse Hh pathway depends upon the presence of the primary cilium[6].

Despite the conserved role of Cos2/KIF7 in the Hh pathway, the motor domain of Cos2 lacks residues critical for motility[17] and is considered as a microtubule-associated scaffold for Hh signaling complexes [18,19]. In contrast, mouse KIF7 has the sequence motifs necessary for ATP and microtubule binding and the crystal structure of its motor domain is superimposable on that of a conventional kinesin [20]. How KIF7 acts within cilia and whether its motor activity is important for its function is not known.

Here we show that, unlike other core components of the mammalian Hh pathway, KIF7 is required for the normal structure of primary cilia. KIF7 localizes to the distal tips of primary cilia, the site of the plus-ends of axonemal microtubules. In the absence of KIF7, cilia are long and unstable. Using TIRF microscopy-based *in vitro* assays, we show that a purified KIF7 motor protein can autonomously recognize microtubule plus-ends and limit growth; these growth-limiting activities are sufficient to explain the long cilia of *Kif7* mutants. Proteins that normally localize to distal cilia tips, including the Gli and Sufu proteins that mediate Hh signaling, are found in ectopic puncta along the *Kif7* mutant cilium. The data suggest that KIF7 is required to organize a specialized compartment at the tip of the cilium that is necessary for Hh signal transduction.

Results

KIF7 localizes to cilia tips

We found that endogenous KIF7 was enriched in primary cilia tips in Sonic hedgehog (Shh)-responsive cells in wild-type embryos (Fig. 1a–b) and cultured fibroblasts and was further enriched at tips in response to activation of the pathway (Fig. 1c–d; Supplementary Fig. 1b), similar to the core Hh pathway proteins Gli2, Gli3 and Sufu [21–24]. KIF7 was also present at cilia tips in MEFs derived from mutant embryos that lack Smo or Gli2 and Gli3, indicating that KIF7 is targeted to cilia independently of Shh pathway proteins (Supplementary Fig. 1c–d). In wild-type MEFs, KIF7 was present at cilia tips at all stages of

ciliogenesis (Fig. 1e). No KIF7 protein was detected in cilia of mouse embryonic fibroblasts (MEFs) derived from *Kif7*$^{-/-}$ embryos [8] (Fig. 1f; Supplementary Fig.1a). An allele of *Kif7* with a leucine-to-proline substitution (L130P) in a conserved region of the motor domain causes a phenotype indistinguishable from that of the null allele [6]. KIF7 protein level was not affected in *Kif7*^{L130P} MEFs, but KIF7 was never observed at tips of *Kif7*^{L130P} mutant cilia, although it was detected in the ciliary transition zone (Fig. 1f; Supplementary Fig. 1a–b).

Kif7 mutant cilia are long and twisted

Cilia were present on ~70% of *Kif7*^{L130P} and *Kif7*$^{-/-}$ mutant MEFs, as in wild type, but the cilia appeared to be longer than wild type (Fig. 1f–g; Supplementary Fig. 1e–f). Using Arl13b as a cilia marker [25], wild-type MEF cilia were 2.80±0.47 μm in length, whereas mutant cilia were 3.58±1.14 μm and 3.46±1.10 μm in *Kif7*^{L130P} and *Kif7*$^{-/-}$ MEFs, respectively. Thus *Kif7* mutant cilia were ~30% longer, on average, and more variable in length, than wild type (Fig. 1h).

En face imaging of the embryonic neural epithelium by scanning electron microscopy (SEM) showed that neural cilia in *Kif7*^{L130P} and *Kif7*$^{-/-}$ were longer and more tapered than in wild type (Fig. 1i). The diameter of neural tube cilia in *Kif7*^{L130P} mutant embryos was normal near the base, but the distal region of the cilium was thin, with a diameter ~40% less than wild type, and often twisted (Supplementary Fig. 2a). Cilia in the e8.0 *Kif7*^{L130P} embryonic node showed similar morphological defects (Supplementary Fig. 2b–c). Twisted distal segments of mutant cilia were also seen in longitudinal transmission electron microscopy (TEM) sections (Fig. 1j; Supplementary Fig. 2d). Transverse TEM sections of *Kif7*^{L130P} cilia showed that some axonemal microtubule doublets had open B-tubules or only 8 doublets (Supplementary Fig. 2e).

Kif7 mutant axonemes are under-modified and unstable

Axonemal microtubules are acetylated and glutamylated, modifications associated with stable microtubules [26]. Line-scan analysis of fluorescence intensity revealed that the level of tubulin acetylation and glutamylation were comparable in wild type and *Kif7*^{L130P} at the base of the ciliary axoneme (Fig. 2a–c). However both tubulin modifications faded towards the ciliary tip, and tubulin glutamylation was often undetectable distally in *Kif7*^{L130P} and *Kif7*$^{-/-}$ mutant cilia (Fig. 2b–c; Supplementary Fig. 3).

To test whether changes in tubulin modification were associated with decreased cilia stability, we treated cells with nocodazole to induce microtubule depolymerization. In wild-type MEFs, the length of acetylated α-tubulin-labeled axonemal microtubules was reduced by ~20% at 30 minutes after addition of nocodazole. In contrast, 10 minutes after addition of nocodazole, the *Kif7*^{L130P} axoneme was half as long as at time zero and was barely detectable at 30 minutes (Fig. 2d–e). Cilia disassembly is associated with accumulation of IFT particles [27], which were first detected in wild-type cells 30 minutes after addition of nocodazole. Strong IFT88 staining was apparent in the distal half of the mutant cilia at 10 minutes, and by 30 minutes the *Kif7*^{L130P} cilium appeared to be filled with IFT88 (Fig. 2e). Destabilization of axonemal microtubules by exposure to 4°C also caused more rapid loss of

acetylated-α-tubulin and accumulation of IFT88 in *Kif7* mutant cilia than in wild type (Fig. 2f). Thus KIF7 promotes stability of the ciliary axoneme.

KIF7 does not affect the rates of IFT

It has been proposed that cilia length can be regulated by the balance between the rates of anterograde and retrograde IFT[28]. Kinesin-II is the evolutionarily conserved anterograde motor required for carrying intraflagellar transport (IFT) complex from the base of cilia to the cilia tip [29]; other kinesins can also promote anterograde ciliary trafficking and modify the overall rate of IFT [30–32]. To test whether the long cilia in *Kif7* mutants arise because KIF7 alters the rates of IFT, we expressed two fusion proteins, IFT88-GFP to label IFT particles and Arl13b-mCherry to label the ciliary membrane, in MEFs (Fig. 3a) and documented the movements of IFT using time-lapse imaging (Supplementary Movie. 1–2).

We analyzed the speed of IFT trains of wild-type and *Kif7* mutant MEF cilia by measuring the slopes of each IFT trajectory on the kymograph (Fig. 3b). The rates of anterograde IFT were 1.09±0.24 μm/s and 1.06±0.19 μm/s in wild-type and $Kif7^{L130P}$ cilia, respectively. The rates of retrograde IFT were 0.72±0.26 μm/s and 0.76±0.29 μm/s in wild type and $Kif7^{L130P}$, respectively. Thus there was no significant difference in the rates of IFT between wild type and $Kif7^{L130P}$ cilia, indicating that KIF7 does not control cilia length by affecting the rates of IFT.

KIF7 can interact directly with microtubules but lacks detectable motility

Sequence analysis places KIF7 in the kinesin-4 family [33] (Supplementary Fig. 4a), which includes the homodimeric kinesins KIF4A/Xklp1 and KIF21A [1,5,34]. To test whether KIF7 acts as a dimer, we expressed full-length C-terminal Flag- and GFP-tagged KIF7 constructs in HEK293T cells. KIF7-GFP co-immunoprecipitated with KIF7-Flag, and vice versa (Supplementary Fig. 4b), indicating that KIF7 can form a homodimer. When expressed in cell lines, KIF7-GFP appeared to co-localize with microtubule bundles, suggesting that KIF7 can associate with microtubules *in vivo* (Supplementary Fig. 4c). Domain mapping of KIF7 showed that microtubule association and KIF7 dimerization depended on both motor domain (amino acid 13–357) and the first coiled-coil of KIF7 (amino acid 487–539; Supplementary Fig. 4c–d).

To define the biochemical functions of the KIF7 motor, we expressed and purified a recombinant construct in *E. coli* that included the N-terminal motor domain and the first coiled-coil of KIF7, with a C-terminal GFP tag ($KIF7_{560}$-GFP) (Fig. 4a; Supplementary Fig. 5a). We used a TIRF microscopy-based assay to examine the association of $KIF7_{560}$-GFP with microtubules (Fig.4b). In the presence of MgATP (1 mM), $KIF7_{560}$-GFP uniformly decorated the entire microtubule (Supplementary Fig. 5b) and binding was proportional to motor protein concentration (Fig. 4c). Addition of 2 mM AMP-PNP, a non-hydrolyzable ATP analog that typically promotes tight kinesin-microtubule binding, resulted in a ~two-fold increase in filament-bound KIF7 (Fig. 4c; Supplementary Fig. 5b).

We tested whether KIF7 can move along microtubules by analyzing the behavior of single molecules of $KIF7_{560}$-GFP in our TIRF-microscopy assay (Fig. 4b and 4d). Analysis of

kymographs revealed that in the presence of 1mM MgATP, $KIF7_{560}$-GFP molecules were stationary when bound to microtubules, exhibiting neither unidirectional movement nor significant diffusion along the microtubule lattice (Fig. 4d), unlike most kinesins. Increasing the ionic strength of the assay buffer reduced binding life-time of $KIF7_{560}$-GFP associated with microtubules (Fig. 4d), similar to other kinesins [35–37].

The KIF7 motor domain inhibits the growth of microtubule plus-ends *in vitro*

KIF4A/XKLP1 and KIF21A can regulate microtubule length by altering tubulin polymerization dynamics [1,5]. We tested whether $KIF7_{560}$-GFP could regulate microtubule dynamics using a modified TIRF microscopy-based assay to visualize microtubule polymerization *in vitro*, with stochastic transitions between periods of elongation (growth) and shrinkage (catastrophe) at the ends of the microtubules (Fig. 5a) [4,38]. When $KIF7_{560}$-GFP (1 mM MgATP) was added to the dynamic microtubule assay, there was an increase in the frequency of catastrophe at microtubule plus-ends. The catastrophe frequency (0.25±0.10 catastrophe/minute in the absence of KIF7) increased 36% in the presence of 35 nM KIF_{560}-GFP (0.34±0.10 catastrophe/minute) and 60% in the presence of 70 nM KIF_{560}-GFP (0.40±0.12 catastrophe/minute) (Fig. 5b–c). In the presence of AMP-PNP (2 mM), 70 nM $KIF7_{560}$-GFP had no detectable effect on the catastrophe frequency (0.26±0.11 catastrophe/minute) (Fig. 5b–c). When GMP-CPP-polymerized X-rhodamine-labeled microtubules were incubated in solution with relatively high concentrations of $KIF7_{560}$-GFP (500 nM) and 2mM MgATP for 2–5 minutes and then allowed to bind to a glass coverslip, the microtubules appeared fragmented, as if they had been severed in the middle (Supplementary Fig. 6), suggesting that high concentration of KIF7 might have a destabilizing effect on microtubules.

In addition to promoting catastrophe, KIF7 decreased the rate of microtubule growth in a dose-dependent manner (Fig. 5b). In the presence of 70nM $KIF7_{560}$-GFP (1 mM MgATP), the microtubule growth rate (0.52±0.17 μm/minute) was 35% less than the rate in the absence of $KIF7_{560}$-GFP (0.81±0.24 μm/min) (Fig. 5d). An intermediate growth rate (0.66±0.16 μm/minute) was observed with 35nM $KIF7_{560}$-GFP. In contrast, 70nM $KIF7_{560}$-GFP in the presence of AMP-PNP (2mM) only mildly suppressed microtubule growth (0.71±0.20 μm/minute), suggesting that ATP-hydrolysis contributes to the attenuation of tubulin polymerization by $KIF7_{560}$-GFP. At microtubule minus-ends, neither the catastrophe frequency nor the growth rate was significantly affected by $KIF7_{560}$-GFP (Fig. 5c–d), indicating that $KIF7_{560}$-GFP preferentially regulates microtubule dynamics at the plus-ends.

KIF7 acts at growing microtubule plus-ends

To determine the localization of KIF7 on growing and shrinking microtubules, we analyzed snapshots from near-simultaneous imaging of $KIF7_{560}$-GFP (70 nM; 1 mM MgATP) and X-rhodamine-labeled microtubules. Line scan analysis showed that $KIF7_{560}$-GFP associated preferentially with the GMP-CPP-tubulin seed and the with the tip of the microtubule, while it was barely detected in the region of the newly-polymerized microtubule proximal to the tip (Fig. 6a and 6c; Supplementary Movie S3). Time lapse imaging of $KIF7_{560}$-GFP localization on dynamic microtubules showed that the motor protein tracked the plus-ends of microtubules during the growth phase (Fig. 6c). During the depolymerization/catastrophe

phase of the cycle, $KIF7_{560}$-GFP was not detected at microtubule plus-ends (Fig. 6c), suggesting that KIF7 dissociated from the filament plus-end at the onset of catastrophe. Microtubule tip-associated $KIF7_{560}$-GFP was also observed at growing minus-ends, but at <30% the frequency of plus-ends. In the presence of AMP-PNP (2 mM), $KIF7_{560}$-GFP (70 nM) was observed all along the lattice of dynamic microtubules and there was no preferential association with growing microtubule tips (Fig. 6b and 6d). As microtubule plus-ends are capped by GTP-tubulin and the conformation of GMP-CPP-tubulin is similar to that of GTP-tubulin[39,40], the data suggest that KIF7 associates preferentially with GTP-bound tubulin. Together, our *in vitro* analysis suggests that the plus-end-associated KIF7 promotes catastrophe and inhibits microtubule growth in an ATP-hydrolysis dependent manner.

KIF7 is required for organization of the cilia tip compartment *in vivo*

The ability of KIF7 to associate directly with microtubule plus-ends and limit microtubule growth *in vitro*, together with the localization of KIF7 to cilia tips, suggested that the KIF7 might control the dynamics of the distal ends of axonemal microtubules. Close examination of the IFT kymographs revealed that while moving IFT88-GFP appeared as diagonal lines in the kymographs, there were also vertical lines of IFT88-GFP in the kymographs of *Kif7* mutant cilia (Fig. 3b; Supplementary Fig. 7c–e), which represented stationary IFT88 particles. Retrograde tracks almost always began at distal tip in wild-type cilia, but the *Kif7* kymographs showed that retrograde trafficking frequently initiated from the stationary IFT88 puncta in the middle of the axoneme (Supplementary Fig. 7a–b). Thus the stationary IFT88 puncta in *Kif7* mutant cilia mark compartments that have properties of the normal distal tip.

IFT81, an IFT-B complex protein, binds directly to tubulin dimers and facilitates their incorporation into the microtubule axoneme [41]. In wild-type MEFs, IFT81 was enriched in the distal tip of primary cilia and was barely detected along the axoneme (Fig. 7a), consistent with the expression pattern of GFP-tagged IFT81 in ciliated cells [41]. In contrast, multiple IFT81 puncta were present in $Kif7^{L130P}$ cilia, suggesting that the tip structure of the *Kif7* mutant cilia is defective. These results suggest that some axonemal microtubules in mutant cilia do not extend to the distal tip and that ectopic microtubule plus-ends can organize cilia tip-like compartments (Fig. 7a).

Gli2 and Sufu colocalize with distal tip markers along the *Kif7* mutant axoneme

To understand how these defects in cilia structure affected Shh signaling, we assayed the localization of Shh pathway proteins in mutant cilia. Smo moved into cilia normally in response to the small molecule agonist SAG in both wild-type and $Kif7^{L130P}$ mutant MEFs (Fig. 7b), indicating that KIF7 is not required for trafficking of Smo, consistent with the finding that KIF7 acts genetically downstream of Smo [6,8].

In wild-type cilia, Gli2 is present in cilia tips and is further enriched by pathway activation. In contrast, Gli2 was present in puncta along the ciliary axoneme in the absence of pathway activation in both $Kif7^{L130P}$ and $Kif7^{-/-}$ MEFs (Fig. 7b–c). When treated with SAG, additional Gli2 accumulated along the length of mutant cilia (Fig. 7b–c). Despite elevated

level of Gli2 along the mutant axoneme, less Gli2 was present at the distal tip of *Kif7*^{L130P} cilia than in wild type (Fig.7d). Thus KIF7 is not required for trafficking of Gli2 into cilia, but it does control proper localization of Gli2 within the cilium. Sufu, a negative regulator the Shh pathway, forms a complex with Gli proteins at cilia tips and is further enriched in response to pathway activation [24,42] (Fig. 7b and 7e). In *Kif7*^{L130P} cilia, Sufu was present in multiple puncta in the distal half of the ciliary axoneme where it co-localized with Gli2 (Fig. 7b and 7e), indicating that KIF7 is required to restrict Gli-Sufu complexes to the distal end of the cilium. Double staining showed that IFT81 and Gli2 were enriched at the distal cilia tip in wild-type cilia tip and frequently colocalized in ectopic puncta along the axoneme in *Kif7*^{L130P} cilia (Fig. 7f). Thus in the absence of KIF7, the Gli-Sufu complex and IFT81 localize to ectopic tip-like compartments along the axoneme.

Discussion

Mammalian KIF7 and *Drosophila* Cos2 are both required for the switch of the Gli/Ci from transcriptional repressors to activators in the presence of Hh ligand, but KIF7 acts through the primary cilium, which is not required for *Drosophila* Hh signaling. Our data show that KIF7 has an essential role in cilia structure: mouse KIF7 localizes to the tips of primary cilia, where it controls the length and structure of primary cilia and the localization of Hh signaling complexes through its ability to regulate the dynamics of microtubule plus-ends.

Mouse *Kif7* mutant cilia tend to be long, and are unstable and twisted. Cilia in human *KIF7* mutant fibroblasts are longer than controls [13], indicating that KIF7 has a conserved role in the control of axoneme length. Two other classes of kinesin are known limit cilia length. *Chlamydomonas* kinesin-13 moves into flagella via IFT and depolymerizes microtubules from the flagellar tip [43]. Mouse KIF19A, a member of kinesin-8 family, is thought to use its motor activity to move along axonemes and depolymerize microtubule at the tips of motile cilia[44]. Thus each of these kinesins can control cilia length, but they act through distinct mechanisms.

Our *in vitro* reconstitution studies indicate KIF7 associates with microtubule plus-ends where it limits microtubule length. While other kinesins arrive at microtubule plus-ends either by one-dimensional diffusion (e.g. MCAK [45]) or by directional motility (e.g. XKLP1 [1]), KIF7 neither diffuses nor moves directionally on microtubules under our assay conditions. Instead, our data suggests that KIF7 tracks the plus-ends of growing microtubules by preferential association with GTP-bound tubulin at microtubule tip (Fig. 8a). This tip-tracking behavior is ATP-hydrolysis dependent, which distinguishes it from end-binding proteins like EB1 [46]. At the microtubule plus-ends, KIF7 inhibits the rate of microtubule growth, an activity shared with other kinesin-4 proteins. However, unlike KIF4A/Xklp1 and KIF21A, KIF7 is a catastrophe-promoting factor.

The primary cilium is built on a scaffold of parallel microtubule bundles of nine doublet protofilaments, with the plus-ends at the distal cilia tip. Because KIF7 localizes to cilia tips throughout ciliogenesis and purified KIF7 motor protein can autonomously associate with the plus-ends of growing microtubules, we propose that KIF7 binds directly to the distal ends of axonemal microtubules where it limits the growth of the individual microtubules

during cilia assembly. Because tip-associated proteins are mislocalized along the axoneme absence of KIF7, KIF7 also appears to help synchronize the growth of the nine doublet microtubules (Figure. 8b).

The data show that KIF7 is critical for organization of the compartment at the tip of the cilium, a topic that has long been of interest [47]. The IFT complexes that control cilia elongation must disassemble and reorganize at the tip as they convert from kinesin-based to dynein-based motility in the process called tip turnaround [48]. In *Chlamydomonas*, the mating signaling cascade is initiated from the flagellar tip [49]. In mammals, key regulators of Hedgehog signaling are highly enriched at tips of primary cilia, and it has been inferred that their activity is regulated in this compartment [24,42]. We propose that the ectopic activation of the pathway seen in *Kif7* mutants is due to the ectopic Gli/Sufu complexes away from the cilia tip, where they become inappropriately activated in the absence of ligand (Fig. 8b). Because of its specific actions on microtubules, we propose that the ancestral function of KIF7 was to sculpt the structure of the primary cilium, and that it acted in this context in the Hedgehog pathway in the metazoan ancestor of both *Drosophila* and mammals.

Supplementary Material

Refer to Web version on PubMed Central for supplementary material.

Acknowledgements

We thank Leslie Gunther-Cummins, Peter Satir (Albert Einstein College of Medicine, Bronx, NY), Kunihiro Uryu (Rockefeller University) for assistance with TEM, and Alan Hall for use of a microscope for TIRF imaging. We thank Hisham Bazzi, Angela Parrish and Tim Bestor for helpful comments on the manuscript. We thank Bryan Tsou and Won-Jing Wang for technical support and helpful discussion. We thank C.C Hui (Sick Children's Hospital) for providing *Kif7*$^{-/-}$ mice. We thank Jonathan Eggenschwiler (University of Georgia) and Adrian Salic (Harvard University) for antibodies. We thank Nina Lampen for help with scanning electron microscopy and the Memorial Sloan-Kettering Cancer Center core facilities and the Rockefeller University Bio-Imaging Resource Center for help with imaging. We thank Ronald Hendrickson and Hediye Erdjument-Bromage for help with mass spectrometry. This work was supported by National Institutes of Health grant NS044385 to K. V. Anderson and GM65933 to T. M. Kapoor and the MSKCC Cancer Center Support Grant (P30 CA008748).

References

1. Bieling P, Telley IA, Surrey T. A minimal midzone protein module controls formation and length of antiparallel microtubule overlaps. Cell. 2010; 142:420–432. [PubMed: 20691901]
2. Hu C-K, Coughlin M, Field CM, Mitchison TJ. KIF4 regulates midzone length during cytokinesis. Curr. Biol. 2011; 21:815–824. [PubMed: 21565503]
3. Stumpff J, Wagenbach M, Franck A, Asbury CL, Wordeman L. Kif18A and chromokinesins confine centromere movements via microtubule growth suppression and spatial control of kinetochore tension. Dev. Cell. 2012; 22:1017–1029. [PubMed: 22595673]
4. Subramanian R, Ti S-C, Tan L, Darst SA, Kapoor TM. Marking and measuring single microtubules by PRC1 and kinesin-4. Cell. 2013; 154:377–390. [PubMed: 23870126]
5. van der Vaart B, et al. CFEOM1-Associated Kinesin KIF21A Is a Cortical Microtubule Growth Inhibitor. Dev. Cell. 2013
6. Liem KF, HE M, Ocbina PJR, Anderson KV. Mouse Kif7/Costal2 is a cilia-associated protein that regulates Sonic hedgehog signaling. Proc. Natl. Acad. Sci. U.S. A. 2009; 106:13377–13382. [PubMed: 19666503]

7. Tay SY, Ingham PW, Roy S. A homologue of the Drosophila kinesin-like protein Costal2 regulates Hedgehog signal transduction in the vertebrate embryo. Development. 2005; 132:625–634. [PubMed: 15647323]
8. Cheung HO-L, et al. The kinesin protein Kif7 is a critical regulator of Gli transcription factors in mammalian hedgehog signaling. Sci Signal. 2009; 2:ra29. [PubMed: 19549984]
9. Endoh-Yamagami S, et al. The mammalian Cos2 homolog Kif7 plays an essential role in modulating Hh signal transduction during development. Curr. Biol. 2009; 19:1320–1326. [PubMed: 19592253]
10. Jiang J, Hui C-C. Hedgehog signaling in development and cancer. Dev. Cell. 2008; 15:801–812. [PubMed: 19081070]
11. Ingham PW, Nakano Y, Seger C. Mechanisms and functions of Hedgehog signalling across the metazoa. Nat. Rev. Genet. 2011; 12:393–406. [PubMed: 21502959]
12. Ingham PW, McMahon AP. Hedgehog signalling: Kif7 is not that fishy after all. Curr. Biol. 2009; 19:R729–R731. [PubMed: 19906571]
13. Putoux A, et al. KIF7 mutations cause fetal hydrolethalus and acrocallosal syndromes. Nat Genet. 2011; 43:601–606. [PubMed: 21552264]
14. Dafinger C, et al. Mutations in KIF7 link Joubert syndrome with Sonic Hedgehog signaling and microtubule dynamics. J. Clin. Invest. 2011; 121:2662–2667. [PubMed: 21633164]
15. Huangfu D, et al. Hedgehog signalling in the mouse requires intraflagellar transport proteins. Nature. 2003; 426:83–87. [PubMed: 14603322]
16. Goetz SC, Anderson KV. The primary cilium: a signalling centre during vertebrate development. Nat. Rev. Genet. 2010; 11:331–344. [PubMed: 20395968]
17. Matthies HJ, Baskin RJ, Hawley RS. Orphan kinesin NOD lacks motile properties but does possess a microtubule-stimulated ATPase activity. Mol. Biol. Cell. 2001; 12:4000–4012. [PubMed: 11739796]
18. Sisson JC, Ho KS, Suyama K, Scott MP. Costal2, a novel kinesin-related protein in the Hedgehog signaling pathway. Cell. 1997; 90:235–245. [PubMed: 9244298]
19. Robbins DJ, et al. Hedgehog elicits signal transduction by means of a large complex containing the kinesin-related protein costal2. Cell. 1997; 90:225–234. [PubMed: 9244297]
20. Klejnot M, Kozielski F. Structural insights into human Kif7, a kinesin involved in Hedgehog signalling. Acta Crystallogr. D Biol. Crystallogr. 2012; 68:154–159. [PubMed: 22281744]
21. Haycraft CJ, et al. Gli2 and Gli3 localize to cilia and require the intraflagellar transport protein polaris for processing and function. PLoS Genet. 2005; 1:e53. [PubMed: 16254602]
22. Qin J, Lin Y, Norman RX, Ko HW, Eggenschwiler JT. Intraflagellar transport protein 122 antagonizes Sonic Hedgehog signaling and controls ciliary localization of pathway components. Proc. Natl. Acad. Sci. U.S.A. 2011; 108:1456–1461. [PubMed: 21209331]
23. Wen X, et al. Kinetics of hedgehog-dependent full-length Gli3 accumulation in primary cilia and subsequent degradation. Mol. Cell. Biol. 2010; 30:1910–1922. [PubMed: 20154143]
24. Tukachinsky H, Lopez LV, Salic A. A mechanism for vertebrate Hedgehog signaling: recruitment to cilia and dissociation of SuFu-Gli protein complexes. J. Cell Biol. 2010; 191:415–428. [PubMed: 20956384]
25. Caspary T, Larkins CE, Anderson KV. The graded response to Sonic Hedgehog depends on cilia architecture. Dev. Cell. 2007; 12:767–778. [PubMed: 17488627]
26. Janke C, Bulinski JC. Post-translational regulation of the microtubule cytoskeleton: mechanisms and functions. Nat. Rev. Mol. Cell Biol. 2011; 12:773–786. [PubMed: 22086369]
27. Pan J, Snell WJ. Chlamydomonas shortens its flagella by activating axonemal disassembly, stimulating IFT particle trafficking, and blocking anterograde cargo loading. Dev. Cell. 2005; 9:431–438. [PubMed: 16139231]
28. Marshall WF, Qin H, Rodrigo Brenni M, Rosenbaum JL. Flagellar length control system: testing a simple model based on intraflagellar transport and turnover. Mol. Biol. Cell. 2005; 16:270–278. [PubMed: 15496456]
29. Cole DG. Kinesin-II, coming and going. J. Cell Biol. 1999; 147:463–466. [PubMed: 10545491]

30. Insinna C, Pathak N, Perkins B, Drummond I, Besharse JC. The homodimeric kinesin, Kif17, is essential for vertebrate photoreceptor sensory outer segment development. Dev. Biol. 2008; 316:160–170. [PubMed: 18304522]
31. Morsci NS, Barr MM. Kinesin-3 KLP-6 Regulates Intraflagellar Transport in Male-Specific Cilia of Caenorhabditis elegans. Curr. Biol. 2011; 21:1239–1244. [PubMed: 21757353]
32. Ou G, Blacque OE, Snow JJ, Leroux MR, Scholey JM. Functional coordination of intraflagellar transport motors. Nature. 2005; 436:583–587. [PubMed: 16049494]
33. Miki H, Okada Y, Hirokawa N. Analysis of the kinesin superfamily: insights into structure and function. Trends Cell Biol. 2005; 15:467–476. [PubMed: 16084724]
34. Bringmann H, et al. A kinesin-like motor inhibits microtubule dynamic instability. Science. 2004; 303:1519–1522. [PubMed: 15001780]
35. Brady ST. A novel brain ATPase with properties expected for the fast axonal transport motor. Nature. 1985; 317:73–75. [PubMed: 2412134]
36. Scholey JM, Porter ME, Grissom PM, McIntosh JR. Identification of kinesin in sea urchin eggs, and evidence for its localization in the mitotic spindle. Nature. 1985; 318:483–486. [PubMed: 2933590]
37. Vale RD, Reese TS, Sheetz MP. Identification of a novel force-generating protein, kinesin, involved in microtubule-based motility. Cell. 1985; 42:39–50. [PubMed: 3926325]
38. Bieling P, et al. Reconstitution of a microtubule plus-end tracking system in vitro. Nature. 2007; 450:1100–1105. [PubMed: 18059460]
39. Howard J, Hyman AA. Dynamics and mechanics of the microtubule plus end. Nature. 2003; 422:753–758. [PubMed: 12700769]
40. Howard J, Hyman AA. Growth, fluctuation and switching at microtubule plus ends. Nature Publishing Group. 2009; 10:569–574.
41. Bhogaraju S, et al. Molecular Basis of Tubulin Transport Within the Cilium by IFT74 and IFT81. Science. 2013; 341:1009–1012. [PubMed: 23990561]
42. Humke EW, Dorn KV, Milenkovic L, Scott MP, Rohatgi R. The output of Hedgehog signaling is controlled by the dynamic association between Suppressor of Fused and the Gli proteins. Genes Dev. 2010; 24:670–682. [PubMed: 20360384]
43. Piao T, et al. A microtubule depolymerizing kinesin functions during both flagellar disassembly and flagellar assembly in Chlamydomonas. Proc. Natl. Acad. Sci. U.S.A. 2009; 106:4713–4718. [PubMed: 19264963]
44. Niwa S, et al. KIF19A Is a Microtubule-Depolymerizing Kinesin for Ciliary Length Control. Dev. Cell. 2012
45. Helenius J, Brouhard G, Kalaidzidis Y, Diez S, Howard J. The depolymerizing kinesin MCAK uses lattice diffusion to rapidly target microtubule ends. Nature. 2006; 441:115–119. [PubMed: 16672973]
46. Akhmanova A, Steinmetz MO. Tracking the ends: a dynamic protein network controls the fate of microtubule tips. Nat. Rev. Mol. Cell Biol. 2008; 9:309–322. [PubMed: 18322465]
47. Dentler WL, Rosenbaum JL. Flagellar elongation and shortening in Chlamydomonas. III. structures attached to the tips of flagellar microtubules and their relationship to the directionality of flagellar microtubule assembly. J. Cell Biol. 1977; 74:747–759. [PubMed: 903371]
48. Pedersen LB, et al. Chlamydomonas IFT172 is encoded by FLA11, interacts with CrEB1, and regulates IFT at the flagellar tip. Curr. Biol. 2005; 15:262–266. [PubMed: 15694311]
49. Scholey JM, Anderson KV. Intraflagellar transport and cilium-based signaling. Cell. 2006; 125:439–442. [PubMed: 16678091]

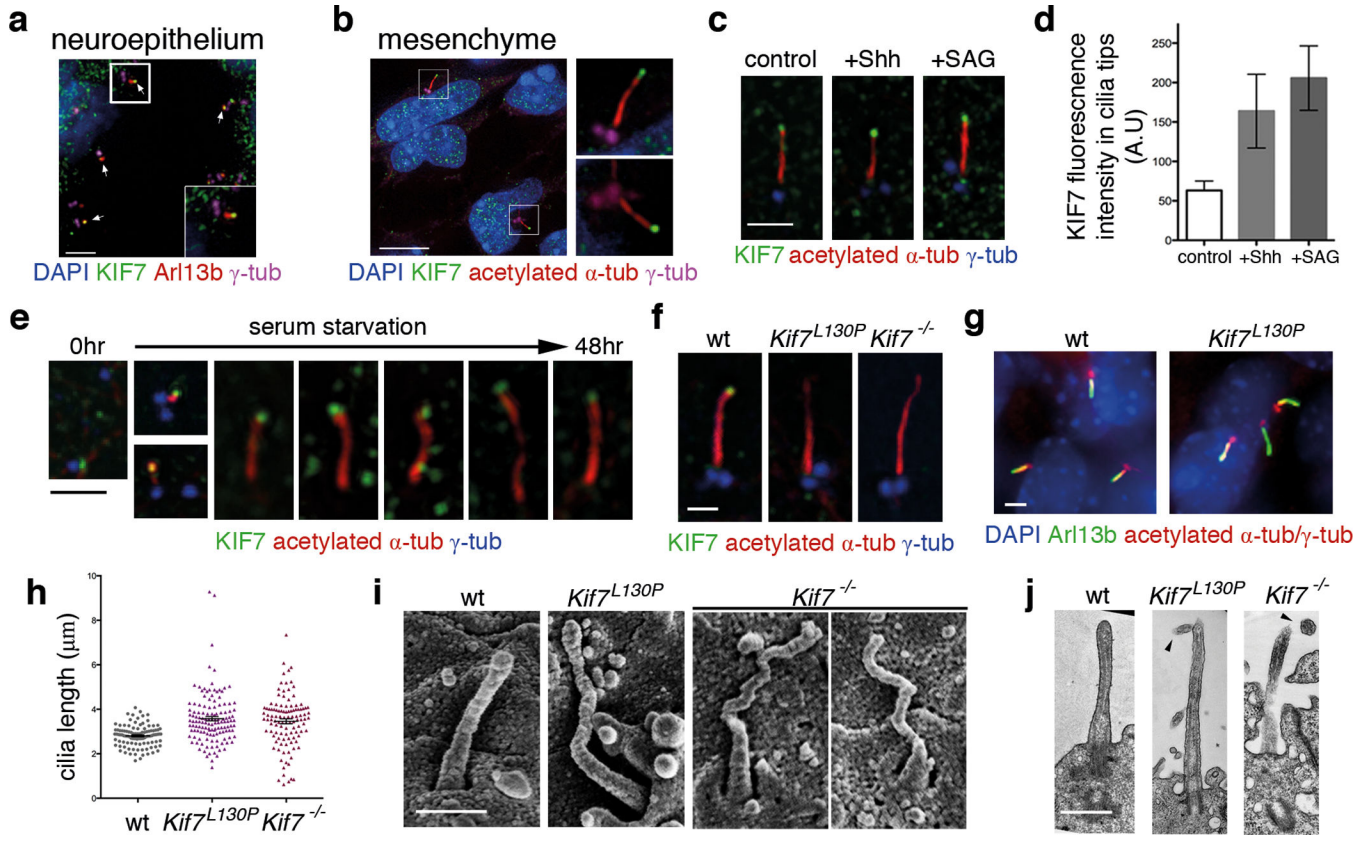

Figure 1. KIF7 constrains the length of primary cilia

(a–b) KIF7 (green) localizes to the tips of primary cilia in e10.5 wild-type embryos. Arl13b (red) marks cilia in (a) and acetylated-α-tubulin (red) marks microtubule axoneme in (b). γ-tubulin (magenta) marks basal bodies. DAPI (blue) labels nuclei. Scale bar = 5μm. (c) In wild-type MEFs, KIF7 (green) is enriched in tips of primary cilia upon treatment with Shh-N recombinant protein (2μg/ml) or SAG (100nM) for 24 hours. Scale bar = 2μm. (d) Quantitation of KIF7 fluorescence intensity shown in (C). n = 150 cilia pooled from 3 independent experiments were counted for each condition. The error bars represent the SD. $p<0.0001$ between control and SAG or Shh treatments by one-way ANOVA. (e) KIF7 (green) is associated with one of the two centrioles prior to ciliogenesis and localizes to the tips of primary cilia throughout cilia elongation induced by serum starvation in wild-type MEFs. (f) KIF7 is not detected at the tips of *Kif7*^{L130P} or *Kif7*$^{-/-}$ MEF cilia. Acetylated-α-tubulin (red) marks primary cilia and γ-tubulin (blue) marks basal bodies in (c), (e) and (f). Scale bar = 1μm in (c), (e) and (f). (g) Primary cilia of wild-type and *Kif7*^{L130P} MEFs stained with Arl13b (green), acetylated-α-tubulin and γ-tubulin (red). DAPI in blue. Scale bar = 2μm. (h) Measurements of MEF cilia length between wild-type and *Kif7* mutants using Arl13b as cilia marker. >100 cilia pooled from 4 independent experiments were counted for each genotype (n=108 cilia for wild type, n=133 cilia for *Kif7*^{L130P} mutant, and n=111 for *Kif7*$^{-/-}$ mutant). $p<0.0001$ between wild-type cilia and *Kif7* mutant cilia by one-way ANOVA. The error bars represent the SEM. (i) Scanning electron microscopy shows neural tube cilia of e10.5 wild-type, *Kif7*^{L130P} and *Kif7*$^{-/-}$ embryos. Wild-type neural cilia were 0.97±0.17 μm and *Kif7*^{L130P} neural cilia were approximately 1.2±0.28μm long (n=50 for

each genotype). Scale bar = 0.5μm. (j) TEM images of longitudinal sections of wild-type, *Kif7*^{L130P} and *Kif7*$^{-/-}$ neural tube cilia. Arrowheads point to twisted tips of mutant cilia. Scale bar = 0.5μm.

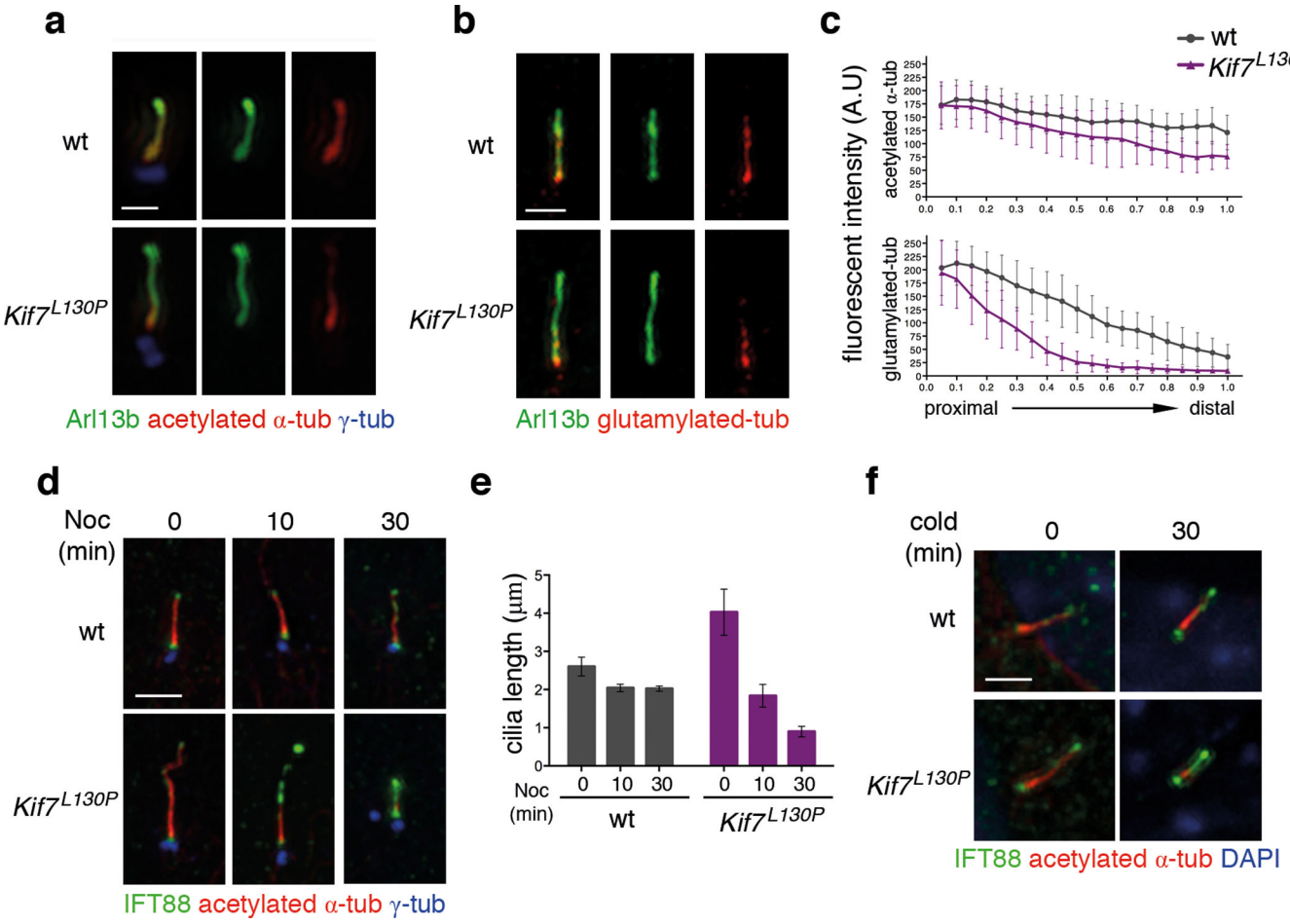

Figure 2. KIF7 stabilizes primary cilia

(a) Tubulin acetylation (red) and (b) glutamylation (red) are reduced at the distal segment of cilia in *Kif7*^{L130P} MEFs compared to wild type. Arl13b (green) labels the entire cilia in (a–b) and γ-tubulin (blue) marks basal bodies in (a). Scale bar = 1μm. (b) Fluorescence intensities of acetylation and glutamylation, as shown in panel (a–b), normalized for cilia length. n= 50 cilia were measured for each genotype pooled from 3 independent experiments. The error bars represent the SD. For tubulin acetylation, $p<0.001$ for the distal half of the cilia. For tubulin glutamylation, $p<0.0001$ for the distal 80% of the cilia. (d) Time course of cilia shortening in response to nocodazole treatment in wild-type and *Kif7*^{L130P} MEFs. IFT88 (green) accumulated distally *Kif7*^{L130P} MEF cilia during cilia retraction. γ-tubulin (blue) marks basal bodies. Scale bar = 2μm. (e) Cilia length was measured using acetylated-α-tubulin from the time-course experiment shown in (d). n=30 for each condition and each time point pooled from 3 independent experiments. The error bars represent the SD ($p<0.001$ between wild-type and *Kif7*^{L130P} at 0 and 30 minutes; n.s between two genotypes at 10 minutes). (f) Time course of cilia retraction at 4°C in wild-type and *Kif7*^{L130P} MEFs. Cilia are marked with acetylated-α-tubulin (red) and IFT88 (green). DAPI in blue. Scale bar = 2μm.

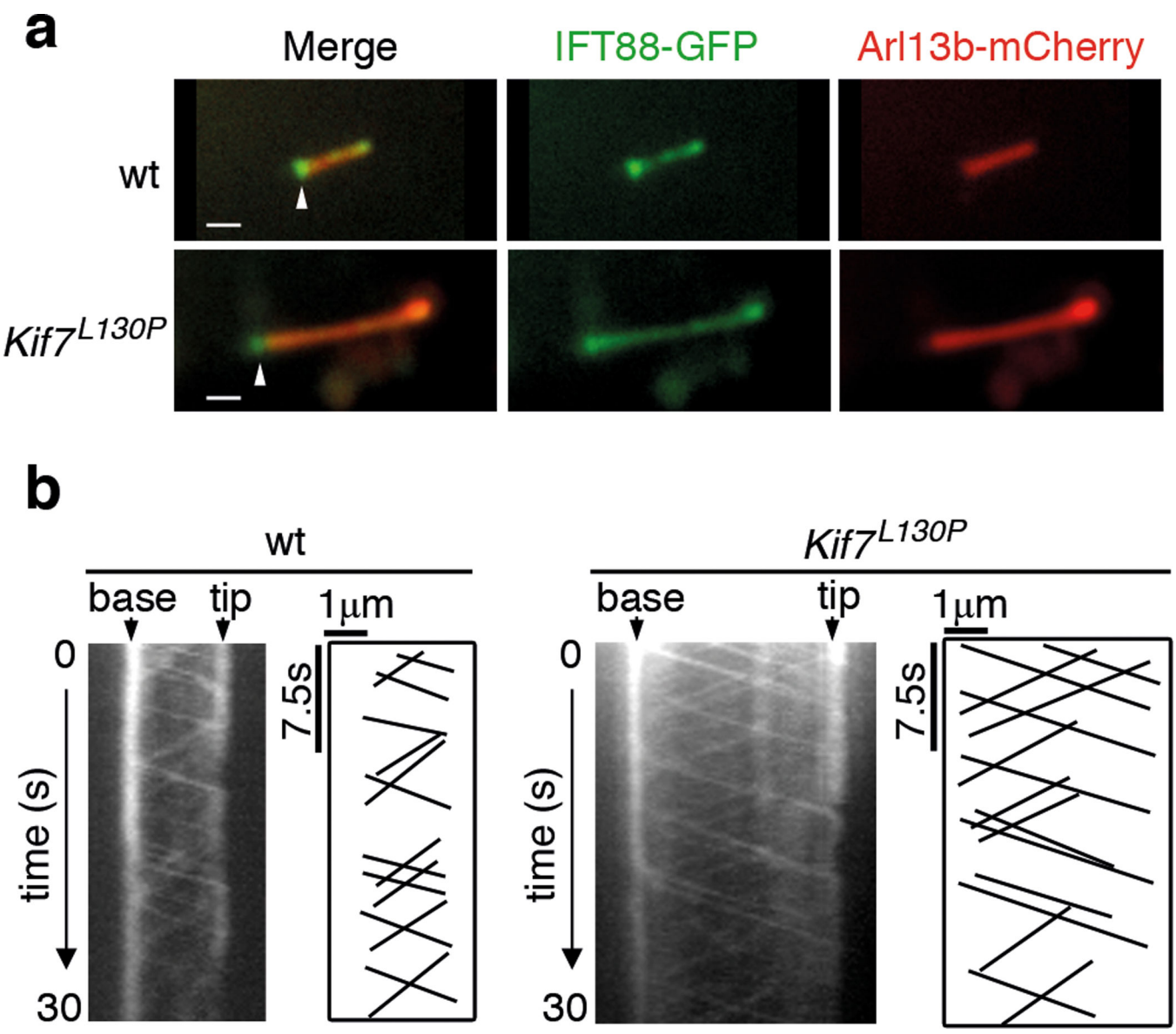

Figure 3. KIF7 does not affect the rates of intraflagellar transport (IFT)

(a) Still images of wild-type and *Kif7*^{L130P} primary cilium expressing IFT88-GFP (green) and Arl13b-mCherry (red) before live imaging. Arrowheads mark the base of the ciliary axoneme. Scale bar = 1μm. (b) Kymographs generated from time lapse imaging of wild-type and *Kif7*^{L130P} primary cilia. Also see Supplementary Movie. S1 and S2. The base and tip of the cilium are indicated with arrowheads. Horizontal scale bar (distance) = 1μm. Vertical scale bar (time) = 7.5 seconds.

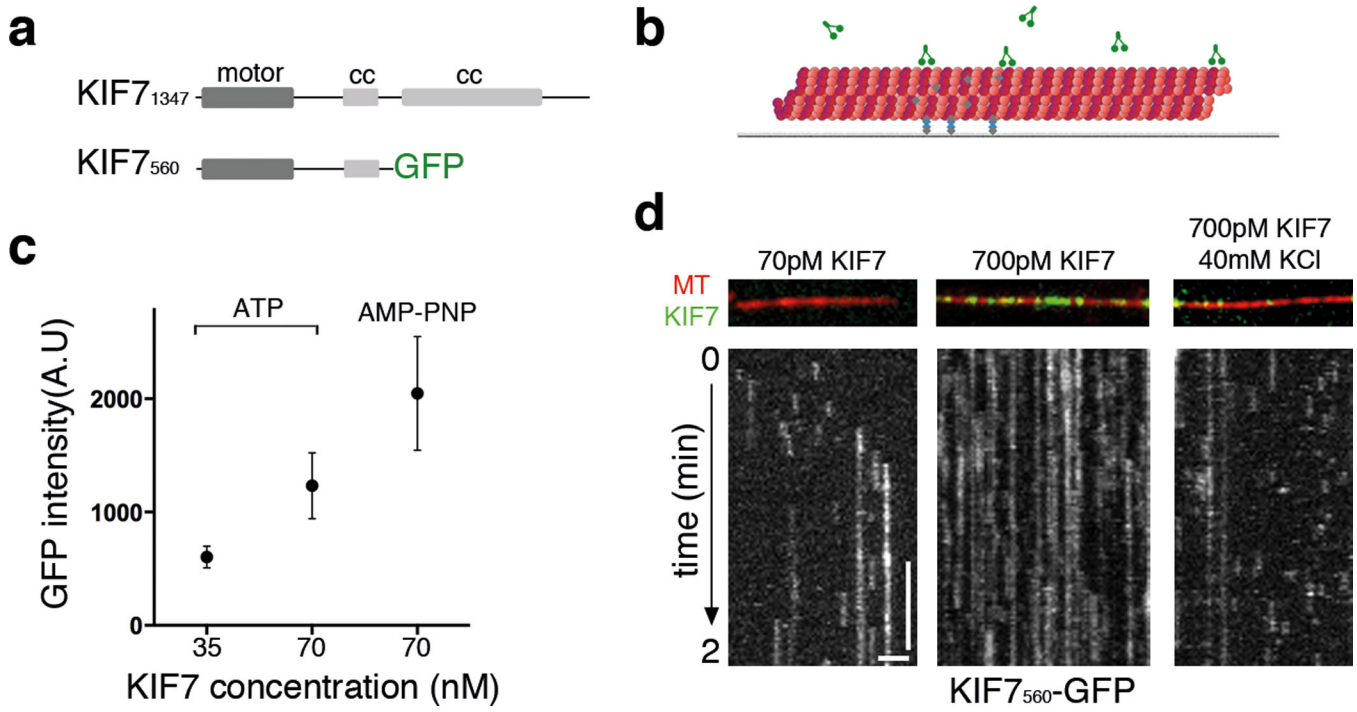

Figure 4. A purified KIF7 motor construct lacks detectable microtubule-dependent motility

(a) Domain organizations of full-length KIF7 and the N-terminal fragment used for *in vitro* assays. (b) Schematic of the assay for examining KIF7-microtubule interaction. X-rhodamine labeled microtubules (red) were attached to a PEG-passivated glass surface by biotin–NeutrAvidin (gray and blue) links prior to addition of KIF7 motor protein (green). (c) Average fluorescent intensity of microtubule-bound $KIF7_{560}$-GFP plotted against KIF7 protein concentration in the presence of either 1 mM MgATP or 2 mM AMP-PNP. n = 20 microtubules for each condition were analyzed. Error bars represent SD. $p<0.0001$ by one-way ANOVA. (d) $KIF7_{560}$-GFP gliding assay (70 pM or 700 pM) under different ionic strength conditions. Representative kymographs from assays at BRB80 and BRB80 +40 mM KCl buffer conditions in the presence of 1 mM MgATP. Still images show $KIF7_{560}$-GFP (green) binding to X-rhodamine labeled microtubules (red). Kymographs of $KIF7_{560}$-GFP are shown in gray scale. Horizontal scale bar = 2μm. Vertical scale bar = 30s. The frame rate was 1 frame per 0.5 s.

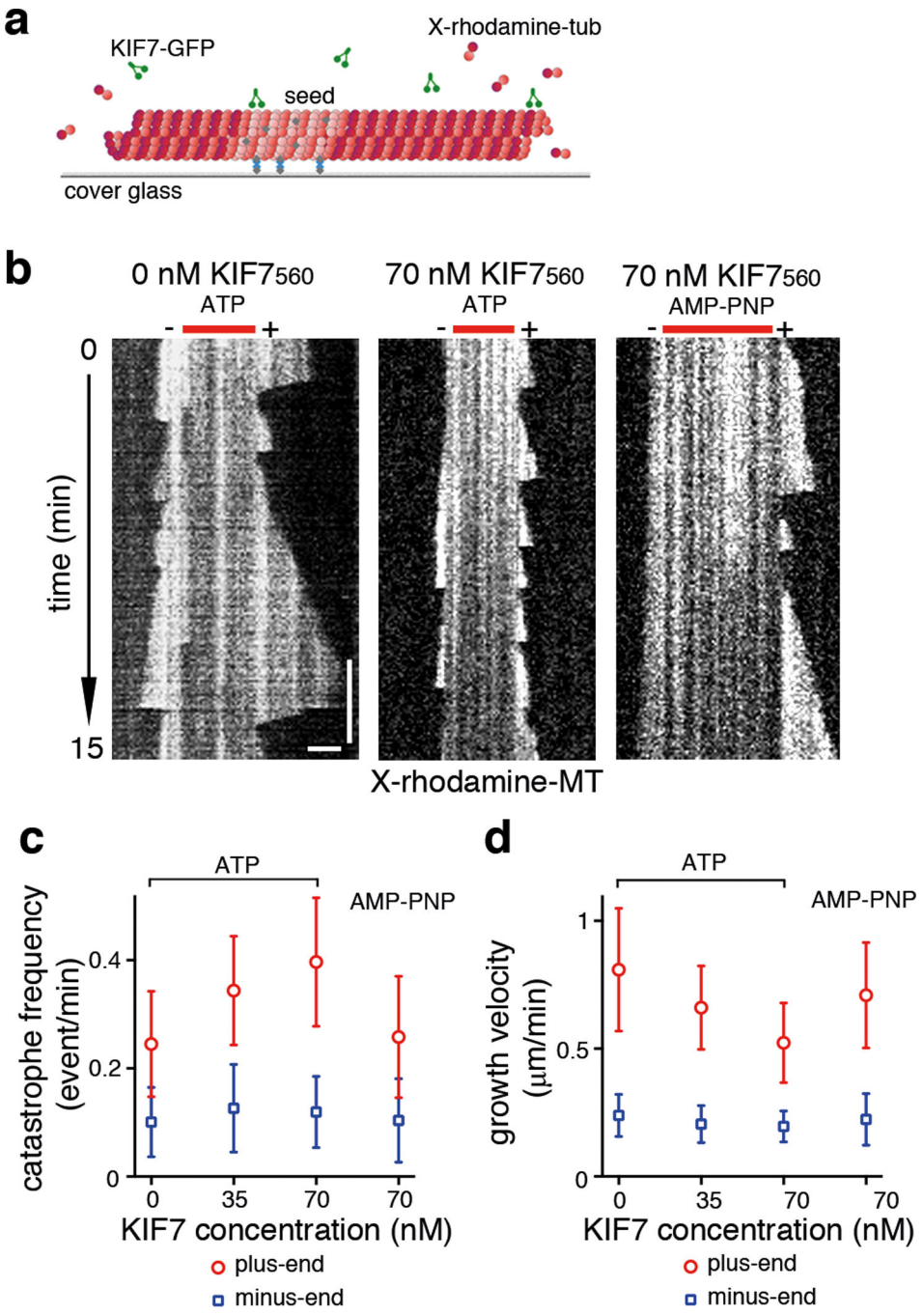

Figure 5. KIF7 alters microtubule dynamics *in vitro*

(a) Schematic of the experimental setup of microtubule dynamics assay: X-rhodamine- and biotin-labeled microtubule seeds, which were polymerized in the presence of GMP-CPP, were immobilized on a glass coverslip, and then incubated with a mixture of X-rhodamine labeled tubulin (1.8 μM) and non-fluorescent tubulin (18 μM; 1 mM MgGTP). (b) Representative kymographs of X-rhodamine-labeled microtubules (show in grey scale) polymerizing in the absence or presence of $KIF7_{560}$-GFP at the indicated concentrations in the presence of either 1 mM MgATP or 2 mM AMP-PNP. The frame rate was 1 frame per

5s. Microtubule seed and polarity are indicated above each kymograph. Horizontal scale bar = 2μm. Vertical scale bar = 180s. (c) The frequencies of microtubule catastrophe in the absence of KIF7 (n=272), 35 nM KIF_{560}-GFP (n=263; $p<0.0001$ compared to control), 70 nM KIF_{560}-GFP (n=492; $p<0.0001$ compared to control and $p<0.01$ compared to 35 nM KIF_{560}-GFP) in the presence of 1 mM MgATP and 70 nM KIF_{560}-GFP (n=179; n.s compared to control) in the presence of 2 mM AMP-PNP were plotted against the $KIF7_{560}$-GFP concentration. The catastrophe frequencies of microtubule minus-ends were not affected by KIF_{560}-GFP (n=82 for control, n=51 for 35nM KIF_{560}-GFP with Mg ATP, n=94 for 70 nM KIF_{560}-GFP with MgATP and n=53 for 70 nM KIF_{560}-GFP with AMP-PNP were analyzed; n.s compared to control). (d) Microtubule growth in the absence of KIF7 (n=145), 35 nM $KIF7_{560}$-GFP (n=109; $p<0.0001$ compared to control), 70 nM (n=263; $p<0.0001$ compared to control and $p < 0.001$ compared to 35 nM $KIF7_{560}$-GFP) in the presence of 1 mM MgATP and 70nM $KIF7_{560}$-GFP (n=101; $p<0.01$ compared to control) in the presence of 2 mM AMP-PNP were plotted against the $KIF7_{560}$-GFP concentration. The growth rates of microtubule minus-ends were not affected by KIF_{560}-GFP (n=51 for control, n=47 for 35nM KIF_{560}-GFP with Mg ATP, n=45 for 70 nM KIF_{560}-GFP with MgATP and n=51 for 70 nM KIF_{560}-GFP with AMP-PNP were analyzed; n.s compared to control). Data sets pooled from 3 independent experiments were analyzed. Error bars represent the SD. p values were calculated by nonparametric test for multiple comparisons.

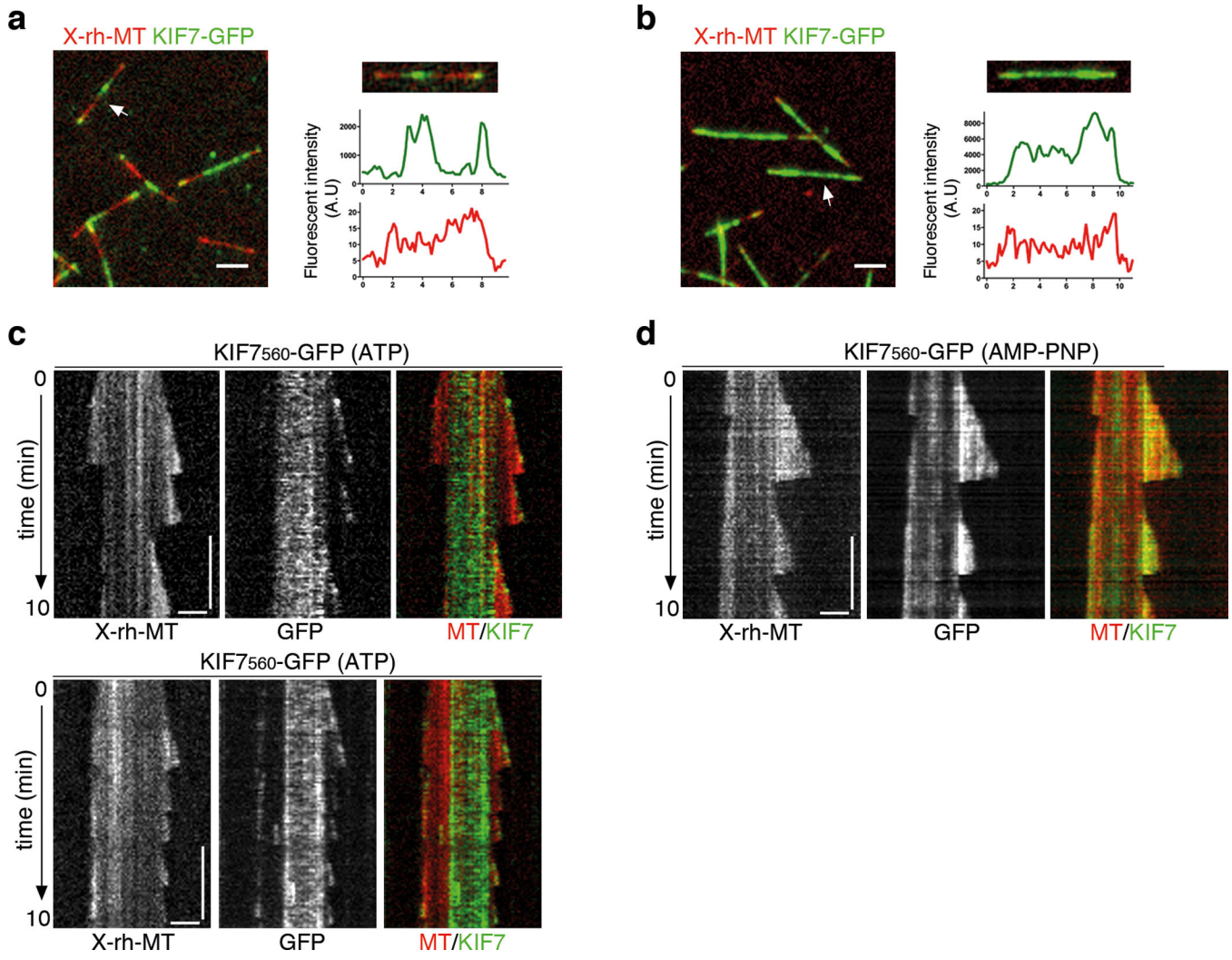

Figure 6. KIF7 tracks microtubule plus-ends

Representative images showing $KIF7_{560}$-GFP (70 nM) associated with dynamic microtubules in the presence of (a) 1 mM MgATP or (b) 2 mM AMP-PNP. Arrows indicates microtubules used for line-scan based fluorescence intensity analysis. Scale bar = 2μm. Also see Supplementary Movie S3. (c) Representative kymographs of $KIF7_{560}$-GFP on X-rhodamine-labeled dynamic microtubules in the presence of 1 mM MgATP (n=263; two examples shown) and (d) 2 mM AMP-PNP (n=101). Plus-ends of microtubules are to the right on the kymographs in (c) and (d). Horizontal scale bar = 2μm. Vertical scale bar = 180s. The frame rate was 1 frame per 5s. Data sets from 2–3 independent experiments were analyzed.

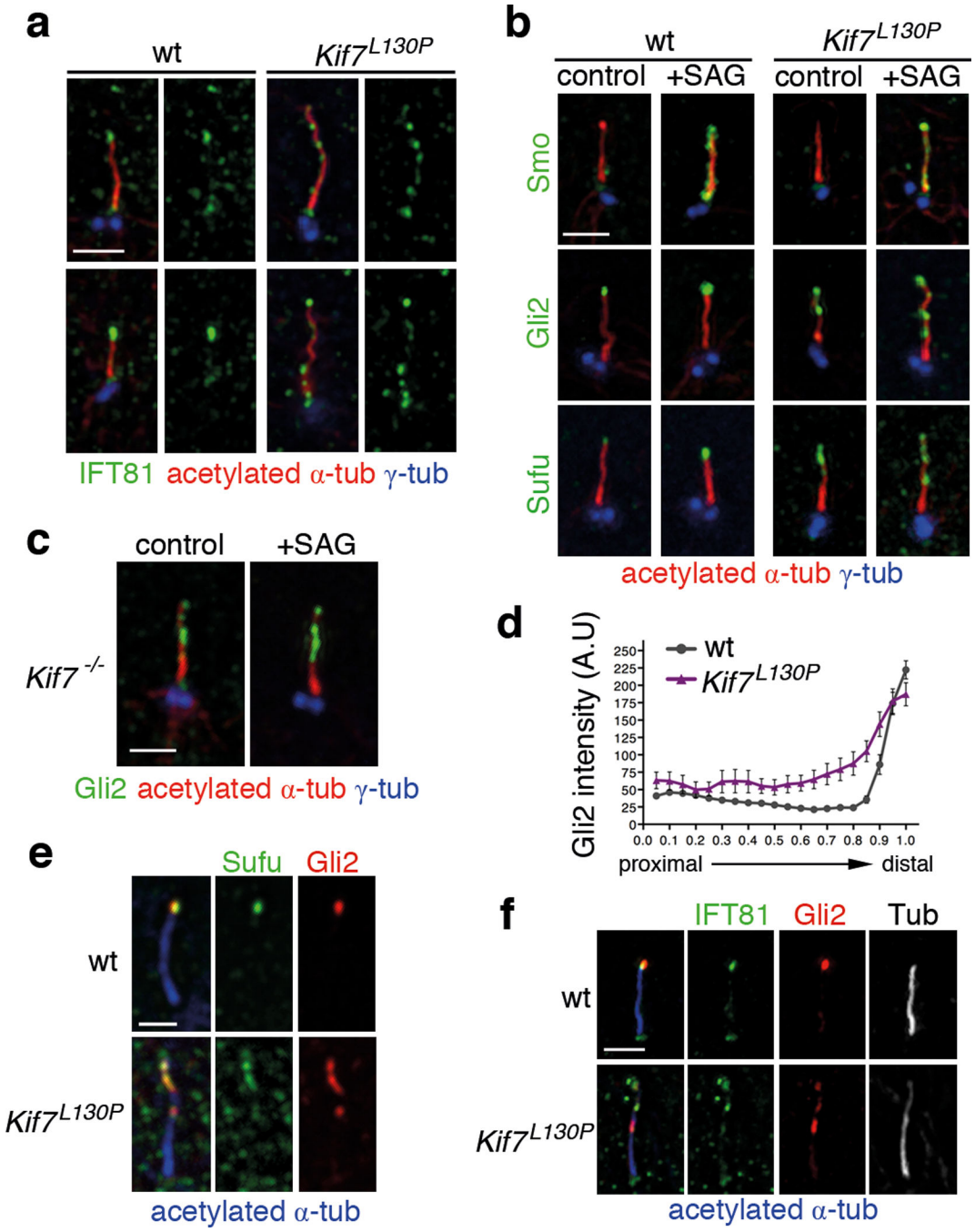

Figure 7. Multiple cilia tip-like compartments form in the absence of KIF7

(a) IFT81 (green) localization in the wild-type and *Kif7*^{L130P} cilia. (b) Cilia localization of Smo, Gli2 and Sufu in wild-type and *Kif7*$^{-/-}$ MEFs in response to pathway activation by 100nM SAG treatment for 24 hr. (c) Gli2 localizes to puncta along *Kif7*$^{-/-}$ ciliary axonemes independent of pathway activation. Acetylated-α-tubulin (red) marks axonemal microtubules and γ-tubulin (red) marks basal bodies in (a) to (c). (d) Distribution of fluorescence intensity of Gli2 in SAG-treated wild-type and *Kif7*^{L130P} cilia, normalized to cilia length. n=50 cilia were analyzed for each condition pooled from 3 independent

experiments. $p<0.0001$. The error bars represent the SEM. (e) Sufu (green) and Gli2 (red) co-localization in the tip of wild-type cilia. In *Kif7*^{L130P} mutant cilia, Sufu and Gli2 co-localize to the same puncta along the axoneme. (f) IFT81 (green) and Gli2 (red) co-localization in the tip of wild-type cilia. In *Kif7*^{L130P} mutant cilia, IFT81 and Gli2 co-localize to the same puncta along the axoneme. Acetylated-α-tubulin shown in blue in merged panels and in gray-scale in separated channels. Scale bars = 1μm in (a)–(c) and (e)–(f).

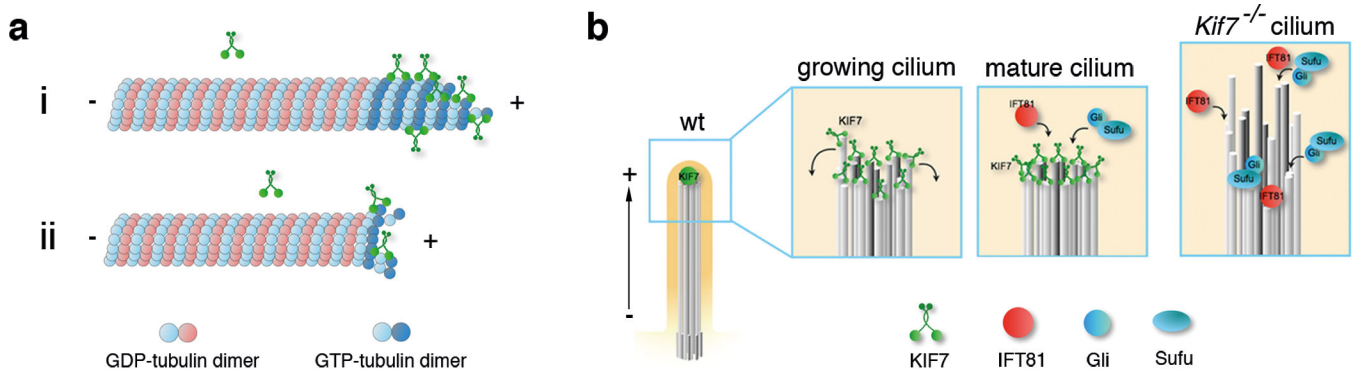

Figure 8. Model for KIF7-dependent regulation of plus-end dynamics in primary cilia

(a) Proposed model for the regulation of microtubule dynamics by KIF7. i: KIF7 preferentially binds to the GTP-bound tubulin at microtubule plus-ends, inhibiting addition of tubulin dimers and microtubule growth. ii: By destabilizing the GTP-bound tubulin cap at microtubule plus-ends, KIF7 can promote catastrophe and thereby limit microtubule growth. (b) Model for KIF7 function at the tip of primary cilia. In wild type, KIF7 acts at the distal end of the growing cilium to prevent overgrowth of individual microtubules and to coordinate the growth of 9-doublet microtubules; only organized microtubule arrays are a suitable substrate for post-translational modifications. In the mature cilium, KIF7 creates a single distal tip compartment where IFT81 and Gli-Sufu complexes are enriched. In the absence of KIF7, growth of axonemal microtubules is not limited and synchronized, leading to longer and unstable cilia and ectopic tip-like compartments that contain IFT81 along the axoneme. Gli-Sufu complexes localized to the ectopic tip compartments, where they can be inappropriately activated in the absence of Shh ligand.